Electric-field effects on H^- photodetachment partial cross sections above 13.4 eV

M. Halka,* P. G. Harris,† A. H. Mohagheghi,‡ R. A. Reeder, C. Y. Tang,* and H. C. Bryant
Department of Physics and Astronomy, The University of New Mexico, Albuquerque, New Mexico 87131

J. B. Donahue and C. R. Quick
Los Alamos National Laboratory, Los Alamos, New Mexico 87545
(Received 15 January 1993)

When static electric fields ($F \leq 90$ kV/cm) were applied to the H^- photodetachment interaction region, new structure and lowered thresholds for production of neutral hydrogen were observed. Relative partial cross sections were measured by detection of excited states of the fragment neutral hydrogen atom H($N=4$, 5, or 6) resulting from laser interaction with relativistic H^- ions. Downward shifts in the onset of excited hydrogen production are observed to increase with field strength, and agree with a recent hyperspherical coordinate interpretation of Zhou and Lin [Phys. Rev. Lett. **69**, 3294 (1992)]. Field-induced window-type resonance structure is observed both below and above the zero-field threshold (ZFT) energy. Quenching of high-lying autoionizing states was also monitored, providing evidence of field-induced tunneling by resonances lying just below the associated ZFT.

PACS number(s): 32.80.Fb, 31.50.+w, 32.80.Cy, 32.80.Dz

I. INTRODUCTION

Experiments investigating the effects of static electric fields on H^- photodetachment thresholds have been limited to energies near the one-electron detachment threshold at 0.7542 eV [1,2]. No resonances are known to exist in this region, and field-induced ripples observed in the cross section near threshold have been described in terms of a time-dependent autocorrelation in the outgoing wave function. Semiclassical closed-orbit theory [3] and frame transformation methods [4,5] have also been successfully applied to this problem, but not to the study of the higher thresholds.

In the experiment reported here the photon energy ranged from 13.4 to 14.2 eV, encompassing the H(N=4,5, and 6) production thresholds. Measured partial cross sections display large downward shifts in the threshold energy in response to applied static electric fields ranging from 0 to 90 kV/cm. These are discussed in Secs. III B and IV A. A partial cross section is proportional to the probability for a photon to detach an electron from H^- and leave the fragment hydrogen atom in a particular N state. (Our detector design did not allow for discrimination among different angular momentum states.) The term "threshold," which is not well-defined in the presence of fields, is here taken to mean the apparent threshold or onset of electron detachment.

At the larger field strengths ($F \geq 50$ kV/cm), interesting structure appears in the threshold regions. In particular, a window-type resonance (dip in the cross section) centered at approximately 13.513 eV, not evident in lower field strengths, is observed in the H($N=4$) continuum channel for F=87 kV/cm (Sec. IV B). This is explained by Zhou and Lin as the field transformation of a Feshbach-type resonance into a shape resonance [6]. Other complicated structures appearing below the zero-field thresholds (ZFTs), probably caused by field-assisted tunneling of zero-field autodetaching resonances, are also explained in their treatment.

Theoretical study of the effect of a field on H^- autoionizing states is still in its infancy. Recent theoretical examinations [7] of the $H^-(n=2)$ shape resonance behavior in applied fields predict lifetime oscillations as a function of field strength. Qualitatively, the predictions may be applicable to high-lying Feshbach resonances, but no rigorous calculations have been carried out for resonances above the $n=2$ series when exposed to external fields. Experiments in the $n=2$ region [8–11] have shown the shape resonance to be quite stable in field strengths up to 3 MV/cm, while the below-threshold Feshbach resonance first splits into Stark-Lo Surdo states, and then quenches in a field of about 2×10^5 V/cm.

Relative total cross sections for the lowest $n=3$ Feshbach state were measured in 1985 [12] in applied fields up to 2.36 MV/cm, where quenching occurred. The results showed no discernible change in width or central energy as the field magnitude was varied.

In this paper we compare widths and energies of resonances recently observed in the H(N=4,5, and 6) continue as a function of field strength (Sec. IV B). Field quenching of the zero-field resonances in this region is discussed in the same section.

II. EXPERIMENTAL METHOD

The basic experimental setup is depicted in Fig. 1. The process is thoroughly detailed elsewhere [13,14], so we give only a brief description here. The 800-MeV H^- beam provided by LAMPF intersects the fourth harmonic (E_{lab}=4.66 eV) of a Spectra Physics DCR-2 Nd:YAG laser at angles α sufficient for photodetachment in an ion's center-of-mass (c.m.) energy range ($E_{c.m.}$) from 13.4 to 14.2 eV, as dictated by the Lorentz transformation

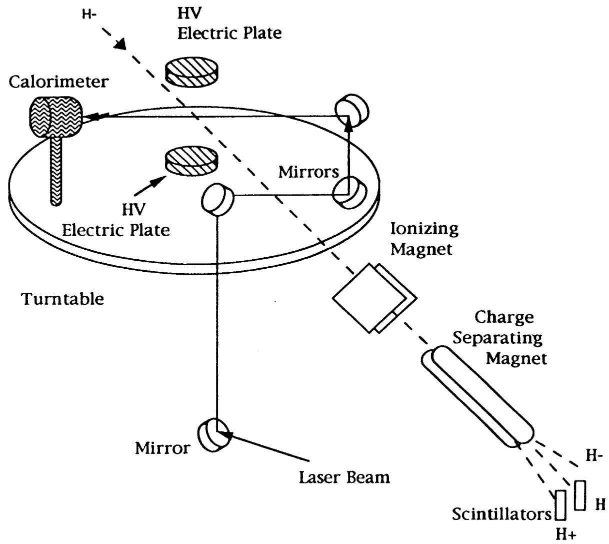

FIG. 1. Diagram illustrating the basic principle of the experiment. Between electric-field plates (HV denotes high voltage) the fourth harmonic (4.66 eV) of the Nd:YAG laser intersects the H^- beam at an angle α which produces the reaction $H^- + E_{\text{c.m.}} \to H(N) + e$. The ionizing magnet produces a field in the H^- center-of-mass frame which strips the $H(N)$ excited state of interest, but not lower energy states. Protons are detected using a scintillation counter after being separated from H atoms and H^- ions by a charge-separating magnet.

$$E_{\text{c.m.}} = h\nu_{\text{c.m.}} = \gamma E_{\text{lab}}(1+\beta\cos\alpha) . \tag{1}$$

β and γ are the usual relativistic quantities, and α is defined to be zero when the beams meet head-on. The laser intensity in the center of mass was about 10^8 W/cm^2. The interaction in the scattering chamber is

$$H^- + h\nu \to H(N) + e^- \tag{2}$$

or

$$H^- + h\nu \to H^{-**}(n) \to H(N) + e^- \tag{3}$$

in static electric fields up to 90 kV/cm, applied perpendicular to the H^- beam using two stainless-steel plates situated above and below the interaction region. These laboratory fields transform to larger fields in the frame of the ion according to $F_{\text{c.m.}} = \gamma F_{\text{lab}}$. H^{-**} is an autoionizing state described in Sec. III C. Since the photon carries one unit of angular momentum and the H^- ion entering the chamber is in its $^1S^e$ ground state, according to electric-dipole selection rules the final state is always $^{2S+1}L^{\pi} = {}^1P^o$, where π is the parity and S is the total spin of the two electrons.

The excited neutral hydrogen atoms $H(N>1)$ formed by the photodetachment of H^- are field stripped and detected as protons downstream in a scintillation counter. An ionizing magnet located between the scattering chamber and the detector allows the selection of the specific N state to be monitored. For example, at c.m. energies between 13.50 and 13.80 eV, only H atoms with the principal quantum number $N \le 4$ are produced [15]. The ionizing magnetic is set to a field which strips H(4), but leaves lower-N states unaffected. The resulting protons are deflected by a charge-separating magnet into a separate counter from the neutral atoms, and constitute the signature for photodetachment when observed in coincidence with a laser pulse. At higher photon energies, hydrogen atoms with $N=5$ and 6 were counted in a similar manner.

The data from different runs were combined and binned in 2-meV-wide bins after normalization to H^- beam current and laser intensity. The cross section σ at each angle α is given by

$$\sigma = GR\frac{\beta\sin\alpha}{IJ(1+\beta\cos\alpha)} , \tag{4}$$

where I and J are the H^- and photon currents, and R is the rate of H production. The $\beta\sin\alpha/(1+\beta\cos\alpha)$ factor accounts for the changing c.m. photon flux and beam overlap with change in angle α. G is a geometrical factor which depends on the spatial and temporal overlaps of the beams. Since we are unable to determine these overlaps in our experiment, G is treated as an arbitrary constant, and our cross sections are relative. Energy calibration was accomplished by monitoring laser-effected transitions between excited states of neutral hydrogen [13]. Our instrumental resolution was determined from the width of the hydrogen lines to be 0.008 eV.

III. THEORY

A. Zero-field thresholds

According to Gailitis and Damburg [16], when no external electric field is present the amplitude A for detachment near threshold is given to first order by

$$A \propto k^{\lambda+1/2} , \tag{5}$$

where λ is the effective angular momentum of the electron pair, $k=\sqrt{2M(E-E_{\text{thr}})}$, and M is the reduced mass. The influence of the long-range dipole $[V_D = -a/(2r^2),\ a<\frac{1}{4}]$ from the excited "core" H atom results in an imaginary exponent, $\lambda+\frac{1}{2}=i\nu$, so that the cross section σ at threshold is a constant to first order. Higher-order terms do exist, and should cause oscillations in the cross section immediately above threshold [16]. Green and Rau, however, show that the modulating factor is modified by $\exp(-\pi\alpha)$ where $\alpha=\sqrt{a-1/4}$ and a is the dipole moment [17]. They calculated α for the dominant photodetachment channels, and found that the $\exp(-\pi\alpha)$ factor makes the amplitude of the expected

TABLE I. Dipole parameter α relevant to H^- photodetachment accompanied by excitation of $H(n)$ [17].

n	α (a.u.)	$\exp(-\pi\alpha)$
4	4.2671	1.5×10^{-6}
5	6.1191	4.5×10^{-9}
6	7.9184	1.6×10^{-11}

oscillations extremely weak—too small to be observable with our current experimental method (see Table I).

B. Thresholds in applied fields

When H^- is photodetached to $H(N)+e$ in the presence of a field the energy onset of detachment may decrease by field lowering of the potential barrier acting upon the outer electron. In zero applied field, the departing electron feels the dipole potential V_D of the degenerate states of the excited H atom it leaves behind,

$$V_D=\frac{-a}{2R^2}\ , \tag{6}$$

where

$$a\approx 3n^2-\frac{23n}{3}+\frac{2}{3n}+1 \tag{7}$$

is the dipole moment for the lowest "+" channel in each manifold (expected to be the dominant channel) [18].

When a field is applied, the outgoing electron also feels the potential from the external field

$$V_F=-Fz\ . \tag{8}$$

The total potential is $V(R)=V_D+V_F$. Letting $z=R$ and setting the derivative with respect to R of $V(R)$ equal to zero obtains

$$V(R)_{\max}=-\tfrac{3}{2}a^{1/3}F^{2/3}\ . \tag{9}$$

If barrier lowering is the only reason for the threshold shift, we expect Eq. (9) to give the magnitude of the shift. It is shown in Sec. IV A that this is close to the experimental value, but not within experimental error.

After examining our data, Zhou and Lin undertook hyperspherical coordinate (HSC) calculations with the hope of understanding the discrepancy [6]. Field deformation of the H^- eigenpotential curves was suspected. They calculated HSC potential curves for the $N=4$ threshold, including only a few, presumably dominant, channels in order to simplify the analysis (see Fig. 2). The potential curves are labeled as +, −, or 0, depending on the motion of the two electrons with respect to the proton and each other [19,20], correlations being strongest in the + mode. Their calculations show that a weak residual coupling between the + and − channels allows the states associated with the + channel to decay through the − channel. The effect is to shift the threshold downward by an amount comparable to the measured value. The comparison is shown in Sec. IV A.

When a field is present the + and − channels no longer converge to the same asymptotic ($R\rightarrow\infty$) limit. Figure 3 shows that for the case of H(4) production, the − curve is lowered in a field $F=87$ kV/cm, while the + curve is raised. The channel coupling—most significant near the crossing point at about $R=45$ a.u.—allows the outer electron in the + state populated by photoabsorption to escape or tunnel through the potential barrier of the − channel. The detachment threshold is thus determined by the barrier height of the − curve, rather than the + curve [6]. This explains why the a value of Eq. (7) does not give the correct result.

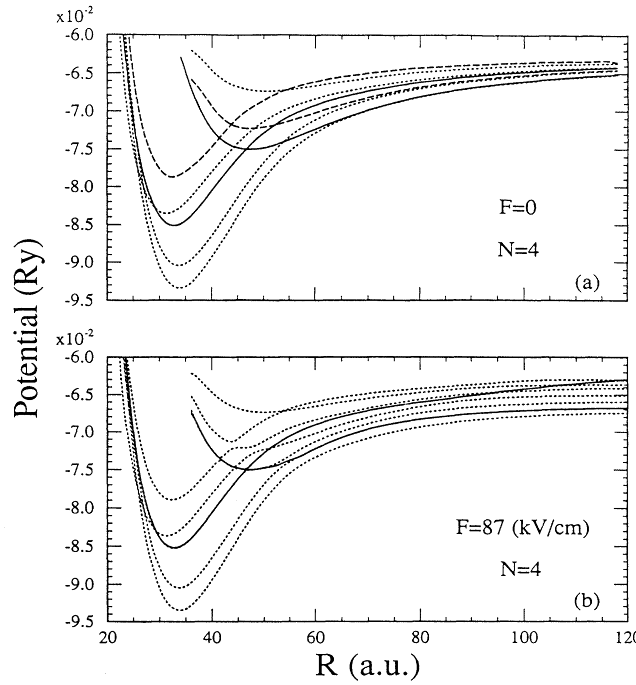

FIG. 2. From calculations of Zhou and Lin [6], hyperspherical potential of H^- as a function of hyperradius R for the $N=4$ manifold. (a) For $F=0$: The two solid lines are diabatic $^1P^o(+)$ (lower line) and $^1P^o(-)$ (upper line) potentials; the two dashed lines are diabatic $^1F^o(+)$ (lower line) and $^1F^o(-)$ (upper line) potentials; the dotted lines, from the bottom, are $^1S^e$, $^1D^e$, $^1G^e$, and $^1H^o(+)$ potentials. (b) For $F=87$ kV/cm: the dotted curves are adiabatic potentials; the lower (upper) solid line is the diabatic curve which converges to the zero-field $^1P^o(+)$ ($^1P^o(-)$) potential at small R.

C. Resonance in applied fields

As the thresholds shift downwards in energy from their zero-field positions, structures (peaks, dips, steps) are observed in the shifted-threshold region. The structure may

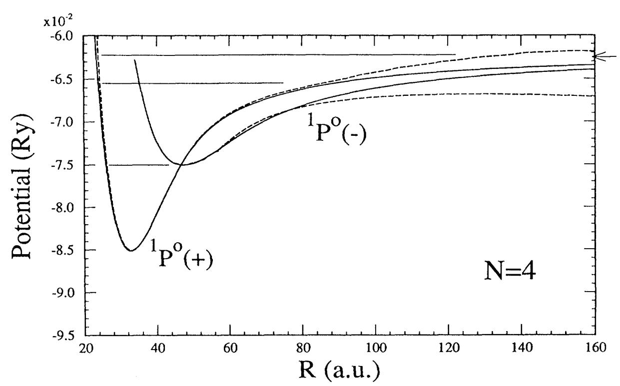

FIG. 3. From calculations of Zhou and Lin [6], comparison between $^1P^o$ diabatic potentials of H^- in $F=0$ (solid lines) and $F=87$ kV/cm (dashed line) for the $N=4$ manifold. The arrow indicates the position of the zero-field threshold. The energy positions of the three lowest resonance states in the $^1P^o(+)$ potential at $F=87$ kV/cm are shown by the horizontal bars.

be partly attributable to field-assisted tunneling of $H^{-**}(n)$ doubly excited Feshbach resonances which converge from below to each $H(n)$ threshold. These are "quasibound" states in which both electrons are excited out of their ground states by a photon with an energy greater than the electron affinity of neutral hydrogen (0.7542 eV), so the resonances exist in the continuum of free electrons. The individual resonances are often labeled as ${}_m(K,T)_n^{A}\,{}^{2S+1}L^{\pi}$ where K, T, and A are approximate quantum numbers describing radial and angular electron correlations [19]. n and m are the principal quantum numbers of the inner and outer electron, respectively.

The resonances decay by "autoionization" to a fragment H atom plus an electron. Here the principal quantum number of the H atom is called N. In zero field the resonances can be observed only in the $H(N \le n-1)$ continuum [21] because the inner electron must exchange energy with the outer electron if autodetachment is to occur. As suggested by Lin [22], however, an external field may supply the outer electron with enough energy to allow autodetachment without affecting the principal quantum number of the inner electron. It would therefore remain in the n level, and the resonance would be observable in the $H(n)$ channel. The following order-of-magnitude calculation shows that fields used in this experiment are of sufficient strength for this process to occur.

Consider for example the ${}^1P^o\ H^{-**}(5)$ state with $n=5$ and $m=7$ below the H(5) threshold. The distance from the inner (outer) electron to the proton is d (s). We take $d=5^2a_o$ [typical $H(N=5)$ atom] and $s=77$ a.u. (from HSC potential curves of Sadeghpour [23]). The field seen by the outer electron is the dipole field of the "core" hydrogen atom

$$F=\frac{ed}{(s+d/2)^3}\approx 30\frac{\text{kV}}{\text{cm}} . \tag{10}$$

So an external field of 30 kV/cm or greater should be sufficient to strip the outer electron, making the resonance observable in the H(5) channel. More detailed calculations of Zhou and Lin explain this behavior in terms of the changing shape of the ${}^1P^o$ potential curves in a field [6].

The same theoretical investigation [6] offers an explanation of the change appearing in a field of 87 kV/cm in the $H(N=4)$ cross section, where a dip which is not seen in lower field strengths develops near 13.51 eV. It is suggested that this feature is the result of the modification of the ${}^1P^o$ + potential curve where an effective centrifugal potential barrier is induced when a field is applied [6]. This potential does not modify the positions of the first two resonances associated with the + channel, but the third resonance is lifted to position above the ZFT. The dip is interpreted as the third lowest resonance $[{}_m(K,T)_n^A={}_6(2,1)_4^+]$ associated with the ${}^1P^o$ + potential curve converging to the H(4) threshold.

Although there are no cross-section calculations showing the effect of fields on resonant states for $n>2$, qualitative statements may be made. The zero-field $H^{-**}(n)$ states should decrease in amplitude when a field is applied, simply because the outer electron can tunnel through the lowered barrier. Since the higher-lying states in each resonant series are more loosely bound, they should be diminished and disappear in smaller field

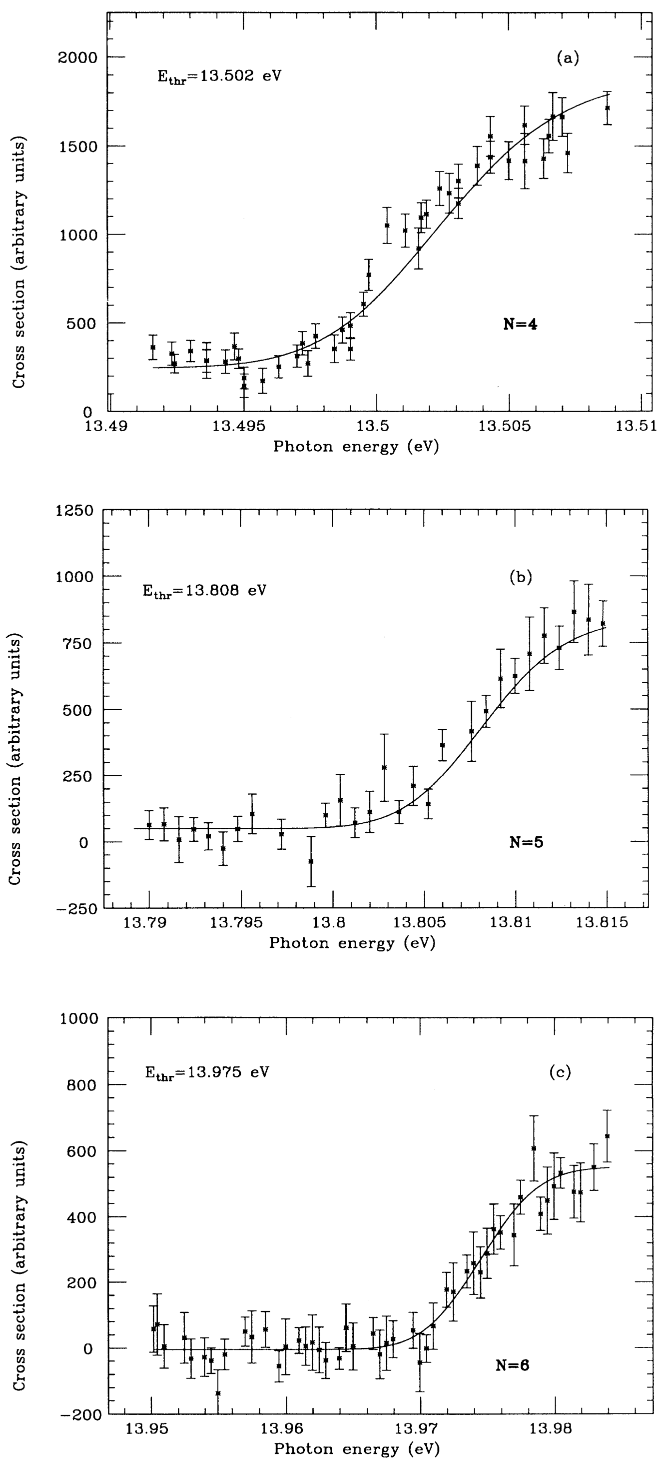

FIG. 4. Thresholds fit to a step function. (a) H(4) threshold, C.L.=0.02%. (b) H(5) threshold, C.L.=95%. (c) H(6) threshold, C.L.= 95%.

strengths than those in the same series that lie lower in energy.

Resonances which do not completely "disappear" should become asymmetric in fields strong enough to cause visible mixing of the $^1P^o$ states with even-parity states, such as $^1D^e$ and $^1S^e$. Spectral repulsion, wherein the Stark states move away from each other, is also expected. A shift in the central energy may be taken as possible evidence of this behavior.

Using R-matrix methods, Slonim and Greene [7] have predicted that the width of the H^- shape resonance ($n=2$) should change with field strength in an oscillatory manner. Feshbach resonances are expected to exhibit the same type of width oscillation. This aspect, as well as quenching and asymmetry of high-lying resonance, has been examined and is reported in Sec. IV B.

IV. ANALYSIS AND RESULTS

A. Measured threshold shifts

The $N=4,5$, and 6 ZFTs were fit to a step function (See Sec. III A) with three parameters: E_{thr}, B, and C,

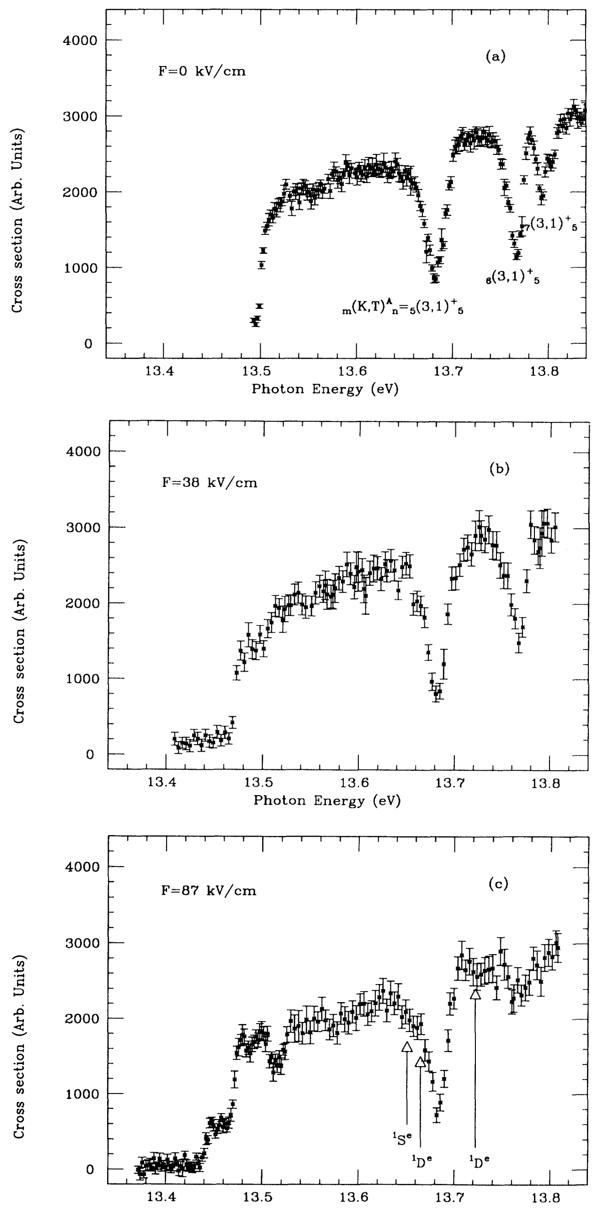

FIG. 5. H($N=4$) relative partial cross section vs photon energy near the $N=4$ threshold for three different field strengths. Error bars are statistical only. (a) No applied electric field. (b) Applied field of 38 kV/cm. (c) Applied field of 87 kV/cm. Arrows point to field-free central energies of some even-parity resonances.

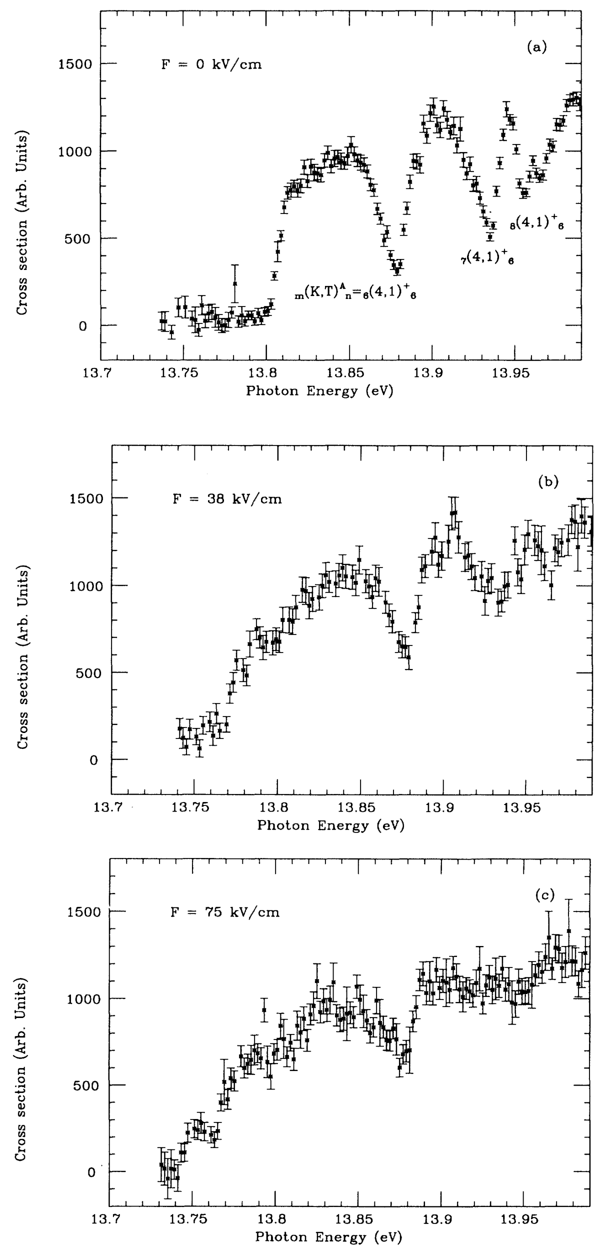

FIG. 6. H($N=5$) relative partial cross section vs photon energy near the $N=5$ threshold for three different field strengths. Error bars are statistical only. (a) No applied electric field. (b) Applied field of 38 kV/cm. (c) Applied field of 75 kV/cm.

where E_{thr} is the threshold energy, B the cross section below threshold, and C the cross section above threshold. The results of fitting the ZFTs to a step function convoluted with a Gaussian function having a width equal to the experimental resolution are shown in Fig. 4. While the $N=5$ and 6 thresholds are good fits to a step function with confidence levels of 95%, the confidence level (C.L.) for the $N=4$ threshold to be a step function is only 0.1%. The poor conformation to a constant function at the H(4) threshold may be an indicator that a centrifugal potential is interfering in this energy region. In fact, a shape resonance centered at around 13.5 eV, dominant in the H($N=2$) decay channel, has been predicted in R-matrix calculations of Sadeghpour, Greene, and Cavagnero [24]. For $n=4$ no shape resonance potential appears in HSC curves of Zhou and Lin, however. The experimental evidence is far from conclusive, but hints that an experimental study with better statistics and better energy resolution might be in order.

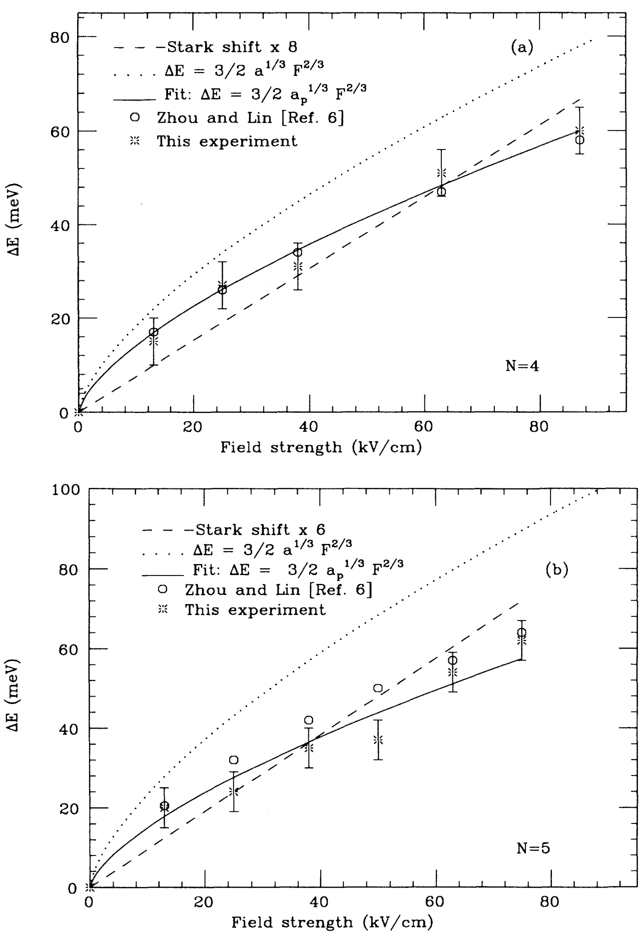

FIG. 7. Threshold shift ΔE relative to the zero-field threshold vs field strength. Solid lines are fits to the function $\Delta E=\frac{3}{2}|a_p|^{1/3}F^{2/3}$ with the dipole moment a_p as a parameter. Open circles indicate values from calculations of Zhou and Lin [6]. Dotted lines are the function $\Delta E=\frac{3}{2}a_p|^{1/3}F^{2/3}$ where a is the theoretical dipole moment for the lowest + channel in the manifold. (a) H(4) threshold shift values. The fit gives $a_p=11.04\pm0.19$ a.u. The dashed line shows that the shifts are 8 times larger than those expected from the first-order Stark effect in H. (b) H(5) threshold shift values. The fit gives $a_p=13.03\pm0.17$ a.u. The dashed line shows that the shifts are 6 times larger than those expected from the first-order Stark effect in H.

H(4) partial cross-section measurements were performed in c.m. field strengths of 0, 13, 25, 38, 63, and 87 kV/cm. The data in Fig. 5 are from 0, 38, and 87 kV/cm runs—sufficient to show the trend with increasing electric field. Most notable is the large shift of the threshold toward lower energies. Figure 6 shows the data for H(5) production in 0, 38, and 75 kV/cm fields. The H(6) field was examined in only two field strengths, 13 and 25 kV/cm. The threshold shifts to lower energies as it does in the other channels, but no unusual structure is observed in the $N=6$ continuum at these field strengths.

The changing shape of the cross section in response to a field made it impossible to ascertain the photon energy for the onset of production by fitting the data to any known function. Therefore, each field-induced threshold energy was chosen to be where the cross section is 13% of its value at 40 meV above the ZFT. The 13% level was selected because it gives values which are consistent with theoretical ZFTs. The reference energy 40 meV above ZFT was chosen in order to avoid field-generated structure. The error in this method was assumed to be ±5 meV—probably an overestimate, as discussed below.

Figure 7 plots the amplitude of the threshold shift ΔE relative to the ZFT for each field strength. These shifts are nearly an order of magnitude larger than those expected from Stark splitting of the H levels, shown by the dashed lines. The solid lines are fits to the function $\frac{3}{2}a_p^{1/3}F^{2/3}$, detailed in Sec. III B. Our fits using the MINUIT [25] code provide $|a_p|=11.0\pm0.2$ (13.0 ± 0.2) a.u. for the $N=4$ (5) threshold, where a_p is the dipole parameter of the relevant photodetachment channel. The χ^2/ν value is less than 0.7 for both fits, implying that we may have overestimated the size of our error bars [26], as mentioned above. These values of a_p are not consistent with theoretical zero-field dipole moments calculated for the lowest + channel in each N manifold: $a=-18.5$ (-37.8) for $n=4$ (5) [from Eq. (9) of Ref. [23]], indicating that the classical interpretation is inadequate. As explained by Zhou and Lin [6], it is found that the coupling between the + and − channels plays a significant role here. Their values for ΔE from quantum-mechanical calculations are plotted as open circles in Fig. 7. Excellent agreement with experiment is seen for the H(4) threshold, while theoretical values are somewhat high compared with the experimentally measured H(5) threshold shifts.

We see no obvious periodic field-induced modulations of the type observed in the H($N=1$) photodetachment threshold [1,2]. One might expect this effect to be present since it is caused by the wave function reflecting from the potential barrier induced by the outgoing electron. We suspect, however, that these modulations or "ripples" in the cross section are being washed out by the presence of resonances. The dipole field in the asymptotic region may also interfere. We also note that the laser used was not well characterized (about 50% π and 50%

σ polarization); ripples might be more obvious if 100% π polarization were used.

B. Observed field effects on resonances

Resonances converging to the $n=5$ and 6 thresholds in fields ranging from 0 to 87 kV/cm were fit to the Fano function [27]. Fano parameters are listed in Table II. Of the three $H^{-**}(5)$ resonances resolved in the experiment, the highest-energy state, ${}_m(K,T)_n^A={}_7(3,1)_5^+$, was quenched by a field of about 87 kV/cm. As remarked in Sec. III C, the resonance may tunnel into the parent channel. One case in particular—that of the second-lowest $H^{-**}(5)$ at about 13.77 eV—seems to verify this idea. In the H(4) channel its energy in an 87-kV/cm field corresponds to a similar feature in the shifted threshold region of the H(5) continuum channel [compare Figs. 5(c) and 6(c)].

The lowest-lying resonance in the $H^{-**}(5)$ series $[{}_m(K,T)_n^A={}_5(3,1)_5^+]$ at $E_0=13.686$ eV is quite asymmetric in an 87-kV/cm field, probably a result of mixing of the ${}^1S^e$ and ${}^1D^e$ states with ${}^1P^o$. [see Fig. 5(c)]. The mixing may also account for slight variations observed in the Fano width and central energy of the resonance as the field magnitude is varied. Small variations in width and resonance energy with field strength are also observed in the second lowest $H^{-**}(5)$ at 13.77 eV and in the two lowest $H^{-**}(6)$ resonances (see Table II).

A particularly intriguing change in the H($N=4$) cross section appears in $F=87$ kV/cm. Figure 5(c) shows that a dip develops which is not seen in lower field strengths. A fit to the Fano function places this feature at 13.513 ± 0.001 eV—10 meV higher in energy than the ZFT. The width from the fit is 15 ± 6 meV. Without explicit cross-section calculations, it is unknown whether this feature should emerge as a peak or a dip, but the field-shifted energy of 13.511 eV calculated by Zhou and Lin using the WKB approximation compares favorably with the central energy of the observed dip.

TABLE II. Fano widths Γ and central energies E_0 for ${}_m(K,T)_n^A$ resonances observed in various static-field strengths F. The error, assigned by our fitting program MINUIT [25], is the deviation from the best-fit value of the parameter that would increase its χ^2 value by 1.

Resonance ${}_m(K,T)_n^A$	F (kV/cm)	E_0 (eV)	Γ (meV)
${}_5(3,1)_5^+$	0.0	13.687(1)	23(1)
	13.0	13.686(1)	21(1)
	25.0	13.687(1)	21(1)
	38.0	13.685(1)	22(2)
	63.0	13.687(1)	24(2)
	87.0	13.688(1)	20(2)
${}_6(3,1)_5^+$	0.0	13.770(1)	17(1)
	2.0	13.771(1)	18(2)
	5.0	13.770(1)	14(2)
	7.0	13.771(1)	14(2)
	10.0	13.768(1)	21(4)
	11.0	13.769(1)	17(3)
	13.0	13.768(1)	22(3)
	25.0	13.769(1)	15(2)
	38.0	13.773(2)	21(4)
	63.0	13.772(4)	21(9)
	87.0	13.780(17)	27(16)
${}_7(3,1)_5^+$	0.0	13.792(2)	20(4)
	2.0	13.792(2)	15(4)
	5.0	13.795(2)	10(2)
	7.0	13.792(2)	12(3)
	10.0	13.791(2)	19(7)
	11.0	13.749(3)	16(1)
${}_6(4,1)_6^+$	0.0	13.881(1)	18(1)
	13.0	13.884(2)	26(6)
	25.0	13.883(1)	17(3)
	38.0	13.882(1)	18(3)
	50.0	13.879(1)	17(3)
	63.0	13.878(1)	22(3)
	75.0	13.881(1)	13(2)
${}_7(4,1)_6^+$	0.0	13.937(1)	15(1)
	13.0	13.933(2)	26(6)
	25.0	13.932(4)	32(14)

V. SUMMARY

In applied electric fields, large, nonclassical shifts to lower energy of the H($N=4$, 5, and 6) production thresholds were observed for the first time. The stronger fields ($F\geq50$ kV/cm) generate resonancelike structure in the cross section below the ZFT region. It has been shown that at least one of these resonances can be attributed to field-assisted tunneling of a Feshbach resonance converging to the ZFT from below. This experimental evidence of "decay to the parent" by an H^- Feshbach state is compatible with results of HSC calculations by Zhou and Lin. A different type of resonance develops *above* the zero-field H(4) threshold energy as the magnitude of the electric field is increased, and is quite obvious in a field $F=87$ kV/cm. This has been interpreted as a field-induced shape resonance [6].

The zero-field Feshbach resonances converging to the H(5,6, and 7) thresholds were observed to shrink and become asymmetric when static fields were applied to the laser-H^- interaction volume. This behavior is in accord with current ideas about the nature of doubly excited resonances, but theoretical cross sections are as yet unavailable.

ACKNOWLEDGMENTS

We acknowledge helpful discussions with Bin Zhou, C. D. Lin, H. R. Sadeghpour, Chris H. Greene, and John Delos. We thank Tom Bergeman for exact calculations of Stark shifts. This work was supported by the U.S. Department of Energy.

*Present address: The University of Tennessee, Knoxville, TN 37996.

†Present address: Nuclear Physics Laboratory, The University of Illinois at Urbana-Champaign, Champaign, IL 61820.

‡Present address: Sandia National Laboratories, Division 7715, Albuquerque, NM 87185.

[1] H. C. Bryant, A. Mohagheghi, J. E. Stewart, J. B. Donahue, C. R. Quick, R. A. Reeder, V. Yuan, C. R. Hummer, W. W. Smith, Stanley Cohen, William P. Reinhardt, and Lillian Overman, Phys. Rev. Lett. **58**, 2412 (1987).

[2] P. G. Harris, H. C. Bryant, A. H. Mohagheghi, C. Tang, J. B. Donahue, C. R. Quick, R. A. Reeder, Stanley Cohen, W. W. Smith, J. E. Stewart, and Carol Johnstone, Phys. Rev. A **41**, 5968 (1990).

[3] M. L. Du and J. B. Delos, Phys. Rev. A **38**, 5609 (1988).

[4] A. R. P. Rau and Hin-Yiu Wong, Phys. Rev. A **37**, 632 (1988).

[5] Hin-Yiu Wong, A. R. P. Rau, and Chris H. Greene, Phys. Rev. A **37**, 2393 (1988).

[6] Bin Zhou and C. D. Lin, Phys. Rev. Lett. **69**, 3294 (1992).

[7] V. Z. Slonim and Chris H. Greene, Radiat. Eff. Defects Solids **122–123**, 679 (1991); I. I. Fabrikant, N.-Y. Du, and A. F. Starace, Bull. Am. Phys. Soc. **38**, 1139 (1993).

[8] P. A. M. Gram, J. C. Pratt, M. A. Yates-Williams, H. C. Bryant, J. Donahue, H. Sharifian, and H. Tootoonchi, Phys. Rev. Lett. **40**, 107 (1978).

[9] H. C. Bryant, David A. Clark, Kenneth B. Butterfield, C. A. Frost, H. Sharifian, H. Tootoonchi, J. B. Donahue, P. A. M. Gram, M. E. Hamm, R. W. Hamm, J. C. Pratt, M. A. Yates, and W. W. Smith, Phys. Rev. A **27**, 2889 (1983).

[10] G. Comtet, C. J. Harvey, J. E. Stewart, H. C. Bryant, K. B. Butterfield, D. A. Clark, J. B. Donahue, P. A. M. Gram, D. W. MacArthur, V. Yuan, W. W. Smith, and Stanley Cohen, Phys. Rev. A **35**, 1547 (1987).

[11] Kenneth B. Butterfield, Ph.D. dissertation, University of New Mexico, 1983 (Los Alamos Report No. LA-10149-T).

[12] Stanley Cohen, H. C. Bryant, C. J. Harvey, J. E. Stewart, K. B. Butterfield, D. A. Clark, J. B. Donahue, D. W. MacArthur, G. Comtet, and W. W. Smith, Phys. Rev. A **36**, 4728 (1987).

[13] P. G. Harris, H. C. Bryant, A. H. Mohagheghi, R. A. Reeder, C. Y. Tang, J. B. Donahue, and C. R. Quick, Phys. Rev. A **42**, 6443 (1990).

[14] Phillip G. Harris, Ph.D. dissertaton, University of New Mexico, 1990 (Los Alamos Report No. LA-11843-T).

[15] As a result of this experiment, it is now known that this is strictly true only for $F=0$.

[16] M. Gailitis and R. Damburg, Proc. Phys. Soc. London **82**, 192 (1963).

[17] Chris Greene and A. R. P. Rau, Phys. Rev. A **32**, 1352 (1985).

[18] H. R. Sadeghpour and Chris H. Greene, Phys. Rev. Lett. **65**, 313 (1990).

[19] For example, see C. D. Lin, in *Few-Body Methods: Principles & Applications,* edited by T. K. Lim, C. G. Bao, D. P. Hou, and H. S. Huber (World Scientific, Singapore, 1986), pp. 507–543.

[20] J. W. Cooper, U. Fano, and F. Prats, Phys. Rev. Lett. **10**, 518 (1963).

[21] Note that for $n \geq 9$ decay to the $H(n-1)$ continuum becomes energetically forbidden in zero field [13,25].

[22] Chii-Dong Lin (private communication).

[23] H. R. Sadeghpour, Phys. Rev. A **43**, 5821 (1991).

[24] H. R. Sadeghpour, Chris H. Greene, and Michael Cavagnero, Phys. Rev. A **45**, 1587 (1992).

[25] F. James and M. Roos, Comput. Phys. Commun. **10**, 343 (1975).

[26] χ^2 is a measure of the spread of the observations divided by a measure of the expected spread. The number of degrees of freedom ν is the number of data points minus the number of fit parameters. χ^2/ν should be approximately unity if the data fits the function well. χ^2/ν less than 1 indicates that error bars have been overestimated. See Philip R. Bevington, *Data Reduction and Error Analysis for the Physical Sciences* (McGraw-Hill, New York, 1969).

[27] U. Fano, Phys. Rev. **124**, 1866 (1961).